Pure & Appl. Chem., Vol. 67, No. 3, pp. 429–436, 1995.
Printed in Great Britain.

Excitonic processes in aromatic molecular crystals of strong exciton–phonon coupling

Atsuo H. MATSUI

Department of Physics, Konan University, Okamoto, Kobe 658 JAPAN

ABSTRACT: We overview our experimental work on exciton self-trapping in simple organic molecular crystals. First we show pressure-induced change in the exciton-phonon interaction, indicating that the interaction depends strongly on the intermolecular distance, and then we demonstrate the experimental results and compare them with theoretical results on the the exciton-phonon coupling constants, presence of the self-trapping barrier, intermediate self-trapped exciton states, the radiative annihilation of excitons at the exit of the self-trapping tunneling process, exciton direct self-trapping rate and direct self-trapping path. Most part of this paper is devoted to show exciton relaxation processes visualized in time-resolved luminescence in Pyrene.

INTRODUCTION

Excimers in organic materials were first addressed by Ferguson for excited-and-unexcited pair molecules in solids (1). Then the concept was widely used to understand a broad Gaussian luminescence band found in dimeric crystals such as pyrene and alpha-perylene in which each lattice point is occupied by a pair of molecules. Excimers are currently recognized as a sort of self-trapped exciton. The theory of interaction between electron and phonons was first developed by Landau (2), and then it was extended to the problem of excitons by several theorists (3)(4)(5)(6). Toyozawa (4) formulated a plain theory considering exciton-acoustic phonon interaction in solids, which provides a double well potential composed of a free and a self-trapped exciton states. In analysing exciton behavior in strong exciton-phonon coupled systems, it is very important to recognize the presence of the self-trapping barrier which separates free and self-trapped states.

EXCITONIC STATES

Intermolecular Distance and Exciton-Phonon Interaction

Simultaneous observation of free and self-trapped exciton luminescence in strong exciton-phonon coupled systems was first suggested by Nishimura and achieved by Luschick in alkali-iodides (7). In organic solids simultaneous observation was first done in pyrene in 1980 (8), and later in alpha- and beta-perylene crystals (9)(10). Interestingly, alpha- and beta-perylene crystals are both composed of the same kind of species, perylene molecules, and differ in crystal structure only. The self-trap depth, the energy difference between the free and the self-trapped states, is shallow (15 cm^{-1}) in beta-perylene but it is deep in alpha-perylene (650 cm^{-1}). The self-trap depth is in good correspondence with the magnitude of the exciton-phonon coupling constant g (11)(12), which is 1.09 in beta-perylene

and 1.61 in alpha-perylene (13). This relationship between g and the self-trap depth strongly suggests that if the exciton-phonon interaction is strong, excitons are self-trapped deeply.

Since the intermolecular distance in beta-perylene is much larger than in alpha-perylene, it suggests that the magnitude of the exciton-phonon interaction g depends on the distance between the nearest neighbor molecules.

The magnitude of the exciton-phonon coupling constant g is plotted against d (or $d_{//}$) in Fig. 1, where d is the shortest intermolecular center-to-center distance in a crystal and $d_{//}$ is the interplaner distance between the nearest plane parallel pair molecules. We will use the value of $d_{//}$ for dimeric crystals, for instance pyrene or alpha-perylene, or for crystals in which the nearest molecules are oriented parallel to each other, for instance in coronene (14) and beta-dichloroanthracene. In Fig. 1, the magnitude of g is found to be smaller than unity in phenanthrene (15), anthracene (16) and tetracene (17). On the other hand, in pyrene (18), alpha- and beta-perylene, coronene (19) and beta-dichloroanthracene (beta-DCA) (20), g is larger than unity and self-trapped exciton luminescence was observed in these crystals.

This diagram suggests that for crystals in which d (or $d_{//}$) ~ 6A, g increases as d decreases and for crystals with d (or $d_{//}$) < 4 A, g decreases as d decreases. This relationship implies that, when d (or $d_{//}$) is as large as 6A, smaller intermolecular distance is favolable to form self-trapped excitons. On the contrary, when d is as short as 4 A, smaller intermolecular distance is no more favolable to form self-trapped excitons, probably because repulsive force between molecules hinder the formation of self-trapped excitons.

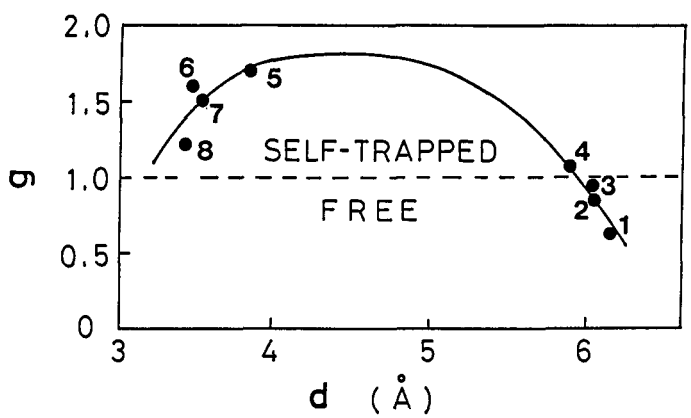

Fig. 1 The exciton-phonon coupling constant g plotted as a function of the intermolecular distance d. 1: Phenanthrene, 2: Anthracene, 3: Tetracene, 4: β -Perylene, 5: β -DCA,6: α -perylene, 7: Pyrene, and 8: Coronene. For definition of the intermolecular distance, see text.

This relationship also implies that if one apply pressure to a crystal, one can change the exciton-phonon coupling constant. Sharp luminescence spectrum of anthracene at 1.5 K changes to broad luminescence band at high pressures (21), indicating that exciton-phonon coupling constant increases with pressure. Similar data are obtained for phenanthrene(22) and tetracene (23). Contrary to these crystals, the couping constant in pyrene (24) and alpha-perylene crystals (25) decreases as expected.

In aromatic molecular crystals the self-trap depth E_{SF} is at most 1500 cm^{-1} (~0.2 eV) and subsequently at room temperature free excitons are in thermal equilibrium with the self-trapped excitons. One can, therefore, estimate the self-trap depth from temperature dependence of the intensity of free exciton luminescence. Once one obtains the magnitude of the self-

trap depth, one can derive the exciton band width 2B using g and E_{SF} values as $2B = (2E_{SF} /(g-1))$. This relationship is very significant in crystals with $g > 1$, because one can determine the exciton band width experimentally. Numerical data reported are summarized in Table I.

TABLE 1. Numerical data for aromatic molecular crystals. In ref (15) and (16), the value of g is not given but it was estimated from the value of the steepness parameter reported therein. The values of E_B, E_{SF}, and 2B are given in cm^{-1}.

	d	$d_{//}$	g	STE	E_B	E_{SF}	2B
phenanthrene	6.16		0.65(15)		non		
anthracene	6.02		0.85(16)		non		
tetracene	6.02		0.95(17)			60	
pyrene		3.53(26)	1.50	yes	300	650	2600
alpha-perylene		3.46(27)	1.61(13)	yes		650	2130
beta-perylene	5.88		1.09(13)	yes		15	
coronene	4.70	3.43(14)	1.22(19)	yes		260	
beta-DCA		3.87(28)	1.66(20)	yes	75	1400	2100

Intermediate Self-trapped State

So-called excimers are illustrative of the deep self-trapped excitons. in pyrene and alpha-perylene crystals As we have seen above, the self-trapped excitons are formed when intermolecular distance is favorable for self-trapping, several molecular conformations are likely for each crystal (29) to exhibit self-trapping. The presence of two types of self-trapped excitons have been reported for crystals such as beta-perylene(30), beta-dichloroanthracene (19), pyrene and alpha-perylene (31). In particular shallow self-trapped exciton states, V and Y states which are stable in pyrene and alpha-perylene respectively below 60 K have been studied in detail(30)(31)(32)(33).

To make discussion simple in this paper we will not discuss excitons in the systems with the intermediate self-trapped state. In the next chapter, we will discuss exciton relaxation processes in crystals which show only one type of self-trapped exciton state.

EXCITON RELAXATION PATHS

Direct and Indirect Self-Trapping Processes

In general, photogenerated excitons in a strong exciton-phonon coupled system can relax to the self-trapped exciton state via two channels. Some of them relax via the bottom of the free exciton band and others relax directly to the self-trapped exciton state without passing the free exciton band bottom. We shall call the former channel as the indirect and the latter as the direct.

While in some materials the indirect process is dominant, while in other materials the direct process is favoured. For example, in Poly(phenylenevinylene) all of the photogenerated excitons relax indirectly (34), but in pyrene in the low temperature phase only the direct process occurs when the photon energy for excitation is larger than the top of the self-trapping barrier (35). In pyrene in its high temperature phase, an intermediate situation is observed: The direct and indirect processes compete.

Recent picosecond spectroscopic techniques visualize exciton relaxation proceses. In what follows, we will discuss the direct and indirect exciton relaxation processes in pyrene in the high temperature phase above 140 K, at which a structural phase transition occurs. In Fig. 2, the adiabatic potential energy curve appropriate for pyrene in the high temperature phase is shown schematically, together with additional information that we will need later.

Before we discuss the direct and indirect processes, we discuss excitons that annihilate radiatively while they slip down the adiabatic potential energy curve. Nasu (36) suggested that optical transition probablity from

the exciton self-trapped state to the ground state varies depending on the initial state within the adiabatic potential of the self-trapped state, and the optical transition probability is large around the exit of the tunneling process. The bottom diagram in Fig. 2 shows luminescence spectrum at 140 K, which is time-integrated over 0-196 ps after photoexcitation at 351 nm (28490 cm^{-1}). A broad band located at 400 nm (25000cm^{-1}) is observed mainly by the optical transition from the exit T of tunnneling process. With a lapse of time the 400 nm luminescence band disappears.

Evidence for Direct Self-Trapping

To see exciton relaxation paths before they reach point T, we have excited a pyrene crystal at two photon energies, 355.6 (28121 cm^{-1})and 376 nm (26600 cm^{-1}), and monitored luminescence at 400 nm (25000 cm^{-1}). The luminescence monitored at 400 nm (25000 cm^{-1}) provides information on the direct and indirect relaxation process depending on the excitation wavelength. For excitation at 355.6 nm (28128 cm^{-1}), excitons are generated well above the band bottom. The luminescence monitored at 400 nm for this excitation includes three kinds of luminescence. One of which is due to exciton that relax directly towards the self-trapped exciton state. This must provide fast decay component. The rest of 400 nm luminescence occurs due partly to excitons that relax first to the free exciton band bottom and they cross over the barrier, and partly due to excitons that annihilate radiatively from the free exciton band bottom to a vibrational level of the ground state. Three kinds of these luminescence processes are shown in Fig. 2(a), (b) and (c).

For excitation at 376 nm (26600 cm^{-1}) only free excitons with wavevector k=0 are generated because the bottom of the free exciton band bottom is located at 376 nm (26600 cm^{-1}). In this case, the luminescence monitored at 400 nm (25000 cm^{-1}) does not include luminescenced due to direct self-trapping of excitons.

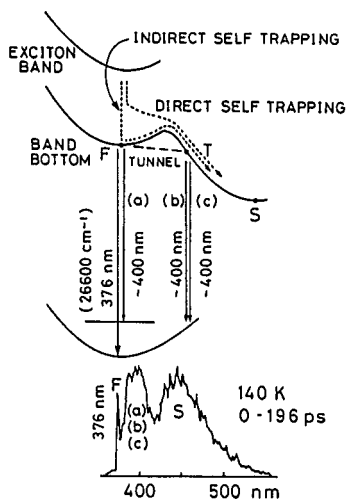

Fig. 2. Simplified diabatic potential energy curve for strong exciton-phonon interaction systems, and used for pyrene at room temperature. The letter 'F' shows the free exciton band bottom and the letter 'S' the self-trapped exciton state. Direct and indirect relaxation paths toward the self-trapped exciton state are indicated. The time-resolved luminescence spectrum shown is obtained at 140 k.

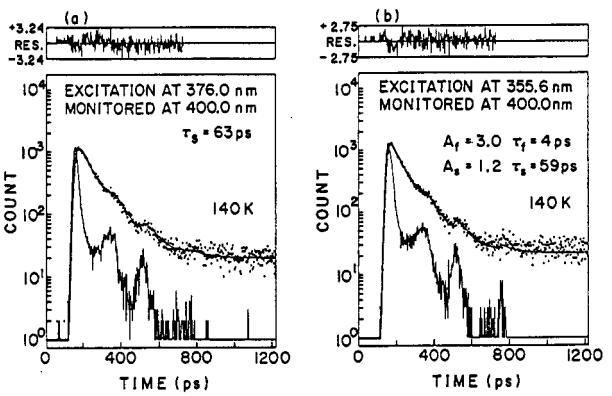

Fig. 3 Luminescence decay curves measured at 140 K and monitored at 400.0 nm (25000 cm^{-1}). (a): Luminescence decay excited at 376.0 nm (26600 cm^{-1}). The decay curve shown at the bottom is an excitation light pulse. The decay time τ_s shown was obtained by convolution analysis. (b) Luminescence decay monitored at 355.6 nm (28120 cm^{-1}). A_f and A_s are respectively the amplitude of the fast and slow decay components.

The decay curves monitored at 400 nm at 140 K are shown in Figs. 3 (a) and (b). For excitation at 376 nm, only a slow decay of 63 ps is observed but for excitation at 355.6 nm two decay components, 4 and 59 ps were found, indicating that both direct and indirect processes occur for high energy excitation. The fractional intensity of the fast decay is plotted in Fig. 4 as a function of the excitation photon energy.

Revised Potential Energy Curve

The adiabatic potential energy diagram shown in Fig. 2 is too simple to discuss exciton relaxation processes in pyrene with the fractional intensity shown in Fig. 4, because it includes only the lowest (singlet) exciton band, although Fig. 2 is very convenient to discuss gross features of excitonic states in aromatic crystals as in Section II, where we have treated excitons that have relaxed already to the free exciton band bottom or excitons in the self-trapped exciton state, it is not adequate to discuss the propaties of excitons immediately after their photogeneration.

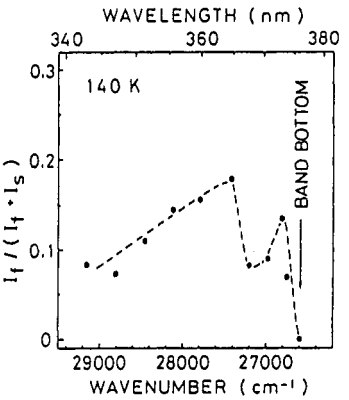

Fig. 4 The direct self-trapping rate, $I_f/(I_f + I_s)$, i.e., the relative intensity, I_f, of the fast decay to the total intensity, $(I_f + I_s)$, as a function of excitation photon energy.

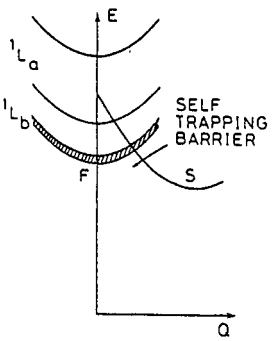

Fig. 5. Revised adiabatic potential energy curve in which the self-trapped exciton state is related to the second singlet excited state, ^1L_a. 'F' and 'S' are respectively the free exciton band bottom and the self-trapped exciton state.

The exciton-phonon coupling constants shown in Table I imply implicitely that they are different crystals and the interaction between excitons and phonons depends basically on individual electronic states of a crystal. Therefore, for precise discussions, we should use the exciton-phonon coupling constant which, as states above, depends on individual excitonic states. It may sometime happen that the coupling constant is larger than unity for one electronic state but smaller than unity for other state. A typical example is coronene crystals at low temperatures, in which the self-trapped exciton state is related to the second excited singlet state and the self-trapped state is located in energy above the lowest excition state (37).

Another similar example is that of pyrene crystals which will be discussed below. The idea of defining the coupling constant associated with an electronic (excitonic) state has originally been pointed out by Azumi (38) and later experimentally by Nozue (39). Nozue has shown that in pyrene $g < 1$ for the lowest exciton band and $g > 1$ for the second exciton band. The self-trap depth for the second exciton band is very deep and consequently the lowest point of the self-trapped exciton state is located well below the lowest exciton band, which is shown schematically in Fig. 5.

The optical trasition from the ground state to the lowest singlet state (^1L_b) is forbidden in pyrene. Therefore, the exciton band width (2B) of the lowest exciton state is very narrow. The second excited state (^1L_a) is also a forbidden state but it has a wide exciton band because it is a

mixed state with an allowed state located near the second forbidden state. As the exciton-phonon coupling is strong for this second forbidden state, excitons get self-trapped deeply as we have mentioned above.

We are now ready to discuss the excitonic relaxation processes using a revised potential energy curve, which is shown in Fig. 5. The direct self-trpping rate, superposed on the adiabatic potential energy curve shown in Fig. 5, is shown by the dot-dashed curve in Fig. 6. It is clear from Fig. 6 that the direct self-trapping rate, $(I_f/(I_f+I_s))$, is large at the excitation photon energy near the ^1L_a band bottom, and at an energy near but below the top of the self-trapping barrier. The direct self-trapping rate is zero for excitation at the ^1L_b band bottom. These results provide a clear evidence that the direct self-trapping rate is related to the electronic excited state.

The direct self-trapping rate in pyrene was calculated by Abe (40), who suggested that the maximum rate is obtained at half of the self-trapping barrier height. Although his theory is developed for 0 K, but the experiments are done at higher temperatures, his theoretical result is quite consistent with our observation that the direct self-trapping rate, $(I_f/(I_f+I_s))$, is large at around the half height of the self-trapping barrier. He also suggested that an increase in optical transition is expected at the photon energy where direct self-trapping occurs. Fig. 7

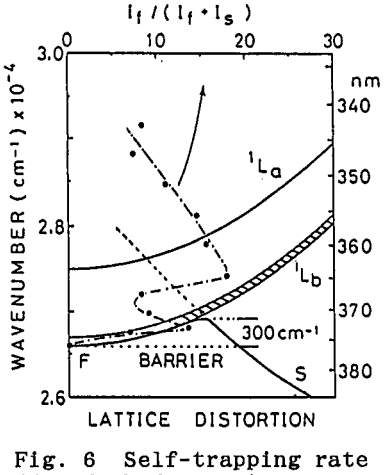

Fig. 6 Self-trapping rate (dot-dashed curve), superposed on the revised adiabatic potential curve for pyrene shown in fig. 5.

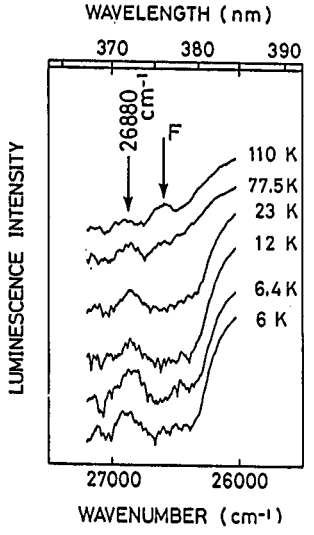

Fig. 7. Luminescence spectra at low temperatures for supercooled pyrene.

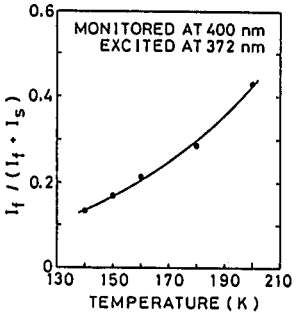

Fig. 8 Temperature dependence of the direct self-trapping rate, $I_f/(I_f + I_s)$ for excitation at 372.0 nm (26880 cm^{-1}).

shows luminescence spectra below 110 K for supercooled pyrene (high temperature phase). There is an luminescence band located at 372nm (26880 cm^{-1}). Its intensity increases upon decreasing the crystal temperature. This luminescence band is located at 220 cm^{-1} above the lowest exciton band marked F. As the self-trapping barier height is 300 cm^{-1} for this crystal, the new luminescence band at 372 nm (26880 cm^{-1}) is probably related to the direct self-trapping. It may also be mentioned here that the intensity of the lowest exciton luminescence band located at 376 nm (26660 cm^{-1}) decreases with decreasing temperature because it is an optically forbidden band.

Temperature dependence of self-trapping rate has been studied theoretically by Ioselvich and Rashba (41). Their theory has been confirmed by an experiment. Fig. 8 shows temperature dependence of the direct self-trapping rate for the excitation at 372.0 nm (26880 cm^{-1}), which is nearly equal to the photon energy at the top of the self-trapping barrier height. The direct self-trapping rate decreases as the temperature is reduced. That means at lower temperatures the number of excitons that reach the ^1L_b band bottom increases.

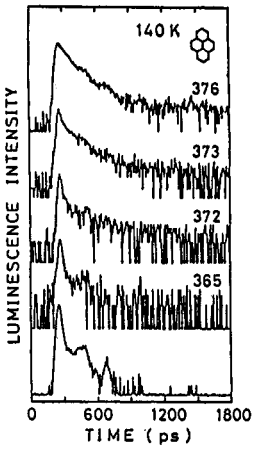

Fig. 9 Luminescence decay curves measuraed at 140 K. The curve shown at the bottom is an excitation light pulse. Luminescence decay is monitored at wavelength shown on the each curve.

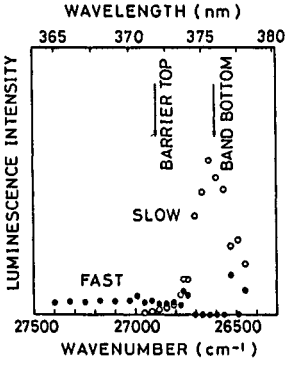

Fig. 10 Luminescence intensity of the fast and slow decay components in pyrene at 140 K. The area under solid circles stands for the luminescence intensity of fast decay component, and the area under open circles for that of the slow decay component.

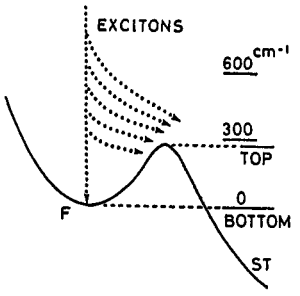

Fig. 11 Exciton relaxation paths, direct and indirect paths for excitons with large kinetic energies. The energy measured from the free exciton band bottom is shown on top.

So far we have discussed excitons that are generated by specific photon energies. To see what happens for excitons with large kinetic energies, hot luminescence has been measured for an excitation at 342.4 nm (29206 cm^{-1}), which corresponds to the photon energy well above the free exciton band bottom. The luminescence decay was monitored at several photon energies in the picosecond time regime. The decay curves, shown in Fig. 9, consist of two components. The intensities (the amplitude multiplied by the decay time) are shown in Fig. 10. Solid circles show the intensity of the fast decay of 4 ps and open circles show that of the slow decay of 35 ps. The energies at the barrier top and the exciton band bottom are shown by arrows.

The fast decay components have been observed in the range between 365 (27937 cm^{-1}) and 374 nm (26738 cm^{-1}). The intensity of the fast component was independent in this wavelength range. When all of the phtogenerated excitons relax to the free exciton band bottom, the intensity of the fast decay component must increase as the monitoring wavelength reaches the band bottom energy, because the number of phonons that scatter excitons increases near the band bottom. However, the observed fact does not agree with this expectation, because it is found to be independent of the wavelength. This result is interpreted in terms of exciton relaxation paths: Most of photogenerated excitons relax directly towards the self-trapped exciton state via various paths and the number of excitons that relax towards the band bottom reduces gradually at the expense of the direct self-trapping. What we have suggested here is shown schematically in Fig. 11.

In Fig. 10, the slow decay component of about 35 ps appears near the band bottom. This shows that excitons which relax close to the band bottom are thermalized. The time of about 35 ps is the time required for excitons to cross over the self trapping barrier, whose height is about 300 cm^{-1}.

CONCLUSION AND ACKNOWLEDGMENTS

We have demonstrated that exciton phonon interaction in aromatic crystals, special emphasis on excitons in pyrene. All those experimental results presented in this paper are quite consistent with theoretical results. In other words, cooperative work with theorists and experimentalists in this research field has been quite fruitful.

We sincerely acknowledge to all of our experimental coleagues and theorists for their valuable suggestions and comments during the course of this work.

REFERENCES

(1) J.Ferguson, J. Chem. Phys. **28**, 765 (1958).
(2) L.Landau: Z. Sowj. Un. **3**, 664 (1933).
(3) E.I.Rashba, Opt. Spectrosk. **2**, 75 (1957).
(4) Y.Toyozawa, Progress in theor. Phys. **26**, 29 (1961).
(5) M.Ueta,H.Hanamura, K.Kobayashi, Y.Toyozawa and E.Hanamura. Excitonic Processes in Solids, Springer Series in Solid-State Sciences, Vol.60 (Springer, Berlin, Heiderberg 1986) Chap. 4.
(6) K.S.Song and R.T.Williams, Self-Trapped Excitons, Springer Series 105 (Springer-Verlag, 1993) p300.
(7) I.L.Kuusmann, P.Kh.Liblik, N.E.Liid'ya, N.E.Lushchik, Ch.B.Lushchik and T.A.Soovik, Sov. Phys. Solid State **17**, 2312 (1975).
(8) A.Matsui and H.Nishimura, J. Phys. Soc. Japan **49**, 657 (1980).
(9) H.Nishimura, A.Matsui and M.Iemura, J. Phys. Soc. Japan **51**, 1341 (1982).
(10) A.Matsui and H. Nishimura, J. Phys. Soc. Japan **51**, 1711 (1982).
(11) H.Sumi and Y.Toyozawa, J. Phys. Soc. Japan **31** 342 (1971).
(12) M. Schreiber and Y. Toyozawa, J. Phys. Soc. Japan **51** 1544 (1982).
(13) A.Matsui, K.Mizuno and M.Iemura, J. Phys. Soc. Japan **51** 1871 (1982).
(14) M.J.Robertson and J.G.White, J. Chem. Soc. 607 (1945).
(15) K.Tomioka, H.Amimoto, T.Tomochika and A.Matsui, Chem. Phys. **59** 4157 (1973). (16) A.Matsui, J. Phys. Soc. Japan **21** 2212 (1966).
(17) K.Mizuno, A.Matsui and G.J.Sloan, J. Phys. Soc. Japan **53** 2799 (1984).
(18) A.Matsui and K.Mizuno, J. Phys. Soc. Japan **51** 3206 (1982).
(19) T.Yamamoto, S.Nakatani, T.Nakamura, K.Mizuno and A.H.Matsui, Chem. Phys. **18** in press.
(20) K. Mizuno, J. Phys. Soc. Japan **59** 1458 (1990).
(21) M.Kobayashi, K.Mizuno and A.Matsui, J. Phys. Soc. Japan **58** 809 (1989).
(22) K.Mizuno, M.Furukawa, and A.Matsui, J. Phys. Soc. Japan **60**, 2768 (1991).
(23) K.Mizuno, A.Matsui and G.J.Sloan, Chem. Phys. **131**, 423 (1989).
(24) A.Matsui and K.Mizuno, Proc. SPIE Intl. Soc. for Opt. Engineering **1054**, 224 (1989).
(25) A.Matsui, T.Ohno, K.Mizuno, T.Yokoyama and M.Kobayashi, Chem. Phys. **111**, 121 (1987).
(26) J.M.Robertson and J.G. White, J. Chem. Soc. 358 (1947).
(27) D.M.Donaldson, J.M.Robertson and J.G.White, Proc. Roy. Soc. A220 311 (1953).
(28) A.Camerman and J. Trotter, Proc. Roy. Soc. A279, 129 (1963).
(29) J.Singh and A.Matsui, Phys. Rev. **B36**, 6094 (1987).
(30) B.Walker, H.Port and H.C.Wolf, Chem. Phys. **92**, 177 (1985).
(31) K.Mizuno, and A.Matsui, J. Lumin. **38** 323 (1987).
(32) R.Seyfang, H.Port, P.Fisher and H.C.Wolf, J. Lumin., **51**, 197 (1992).
(33) H.Sumi, Chem. Phys. **130**, 433 (1989).
(34) M.Furukawa, K.Mizuno, A.Matsui, S.D.D.V.Rughooputh and W.C.Walker, J. Phys. Soc. Japan **58**, 2976 (1989).
(35) M.Furukawa, K.Mizuno, A.Matsui, N.Tamai and T.Yamazaki, Chem. Phys., **138**, 423 (1989).
(36) K.Nasu, J. Lumin., **38**, 90 (1987).
(37) S.Nakatani, T.Nakamura, K.Mizuno and A.H.Matsui, J. Lumin. **58**, 343 (1994).
(38) T.Azumi and S.P.McGlynn, J. Chem. Phys. **41**, 3131 and 3839 (1964).
(39) Y.Nozue, private communication.
(40) S.Abe, J. Phys. Soc. Japan, **59**, 1496 (1990).
(41) A.S.Ioselevich and E.I.Rashba, Solid State Commun., **55**, 705 (1985).